CW IR LIDAR FOR REMOTE MONITORING OF NATURAL GAS LEAKS

R.R. Agishev, L.R. Aibatov, and Yu.E. Pol'skii

A.N. Tupolev State Technical University, Kazan'
Received July 25, 1994

Estimates of top achievable characteristics of the cw IR lidars, together with comparative analysis of various techniques for environmental monitoring are presented. Energy and accuracy characteristics of the analyzed systems are discussed. Principles of designing the cw lidars are overviewed.

1. INTRODUCTION

Currently, there is a persistent interest in applying the lidars to remote monitoring of microconcentration of various gases in atmospheric air. One of the most important tasks consists in analyzing the content of various hydrocarbons, particularly saturated ones, such as methane, ethane, propane, butane, etc., which find extremely wide practical use.

However, application of lidar systems to remote sensing of environment is limited to experimental projects and laboratory prototypes. The problem is that the traditional approach to monitoring of the environment and remote chemical analysis is based on using of pulse lidar systems. Profiling of atmospheric parameters by such systems involves measuring the signal by photodetector at a moment defined by scattered signal delay relatively to sounding pulse.[1,2] Costly high–power pulse lasers used in such systems have cumbersome and unreliable pumping systems, generate a powerful pulse noise, and demand water cooling.

However, there exists an alternative approach to construction of lidar systems, which is specified by energy equivalence between a pulse lidar with high peak output power in its short pulse and a cw lidar with low average output power and long accumulation time. Such continuous wave (cw) gas lidars are much cheaper, and their transmission range is controlled by measuring either the frequency difference between emitted and received signals, or phase difference between these signals.

2. CAPABILITIES AND LIMITATIONS OF CW SYSTEMS

One of the widely used cw lasers is a He–Ne laser. Its two spectrally close transitions $\lambda_0 = 3.3922$ ($3s_2 - 3p_4$ Ne) and $\lambda_1 = 3.3912$ μm ($3s_2 - 3p_2$ Ne) fit into the principal absorption band of many hydrocarbons, thus stimulating the development of systems for remote monitoring, which can be built around such a laser. Below we consider capabilities and limitations typical for such systems.

Note, first of all, that the background concentration of CH_4 in dry air at standard atmospheric pressure and temperature of 273 K in urban environment varies around $N_b = 1$ ppm or $4 \cdot 10^{13}$ cm^{-3}, while the absorption cross section for CH_4 at $\lambda = 3.3912$ μm, σ_{abs}, reaches 10^{-18} cm^2. Thus one may estimate the coefficient of extinction of the sensing radiation due to absorption by CH_4: $\alpha = N_b \sigma_{abs} = 4$ km^{-1}. Under normal conditions even at almost 100% relative humidity, the contribution of water vapor does not exceed 1/20 of the background one by CH_4 (see Ref. 5). Hence in the atmosphere more transparent than a weak fog (at meteorological visibility $V > 1$ km), the atmospheric extinction of radiation emitted in the strongest He–Ne laser line within the 3.39 μm range is mostly determined by methane absorption. In a fog ($V = 0.2, \ldots, 1$ km), one should account for both absorption by methane and scattering.

2.1. Technique of differential absorption

Consider the characteristics of a differential–absorption system for monitoring of methane.[6,7] The power of a signal reflected from a topographic target may be presented in the form

$$P = G P_0 A g \exp(-2\alpha R) t / \pi R^2, \quad (1)$$

where G is the geometric factor; P_0 is the power of sensing radiation; A is the area of the receiver objective; g is the albedo of topographic target; t is the transmission coefficient of the optical system and filters; and, R is the system range.

Not to go into the physical nature of the phenomena taking place in sensors operating above cryogenic temperatures (such as, e.g., PbSe photoresistors), one may assume that the internal noises of such detectors control the threshold power of direct detection as following:

$$P_t = \sqrt{S \Delta F} / D^* \approx 10^{-9} \text{ W}. \quad (2)$$

We estimate the background radiation from daytime sky using the well–known relation[8]:

$$P_b = \pi B_\lambda \Delta\lambda A t \theta^2 / 4, \quad (3)$$

where B_λ is the sky spectral brightness; $\Delta\lambda$ is the transmission bandwidth of the interference filter; and, θ is the plane viewing angle of detector. Assuming $B_\lambda = 10^{-1}$ W/m^2·sr·μm, $\Delta\lambda = 0.06$ μm, $\theta = 3$ mrad, and $A = 0.01$ m^2, we find $P_b \approx 10^{-10}$ W.

One may see that the internal noises of photodetector prevail over the background even for a bandwidth of 10 Hz. Thus the input signal–to–noise ratio of detector, as given by Eqs. (1) and (2), is

$$S / N = G P_0 A g t \exp(-2\alpha R) D^* / \pi R^2 \sqrt{S \Delta F} =$$

$$= 10^3 [\text{km}^2] \exp(-2\alpha R) / R^2 .$$

For a lidar putting out a power around 0.01 W, its signal–to–noise ratio reaches $4.5 \cdot 10^4$ and 0.33, at ranges of 0.1 and 1 km, respectively.

2.2. Lidar technique of differential absorption and scattering

If one follows the lidar technique of differential absorption and scattering (DAS) to monitor gas leaks, the measurement equation has the form

$$P = G\,E\,c\,A\,\beta\exp(-2\alpha R)\,t / R^2, \quad (4)$$

where G is the geometric factor; E is the output radiation energy; β is the volume scattering coefficient: $\beta = i_\pi \alpha$; i_π is the phase function of scattering to angle of π. For flat scattering phase functions, one may follow Ref. 2 and assume, with an error within ±20% suitable for estimating purposes

$$i_\pi = 0.02\ \alpha^{-0.43}. \quad (5)$$

Then

$$P = 0.01\ E\,G\,c\,A\,\alpha^{0.57}\exp(-2\alpha R)\,t / R^2. \quad (6)$$

2.2.1. Direct detection

Operating in the regime of direct detection, the minimum detectable signal is determined similarly to the preceding case, with the only difference that to have the necessary range resolution, one needs a much wider bandwidth ΔF. For $\sqrt{S} = 0.1$ mm, $D^* = 5\cdot10^{10}$ cm $\sqrt{\text{Hz}}$/W, and $\Delta F = 7.5$ MHz ($\Delta R = 10$ m), we find $P_{\min} = 5\cdot10^{-10}$ W. At $V = 10$ km, the signal–to–noise ratio is then equal to

$$S / N = E\,c\,\beta\,A\,t\exp(-2\alpha R)\,D^*/2\sqrt{S}\,\Delta F\,R^2 \approx$$

$$\approx 2.5\cdot10^3\ [\text{km}^2/\text{J}]\cdot E\cdot\exp(-2\alpha R) / R^2. \quad (7)$$

Assuming a discernability coefficient of 10, we find the minimum sensing radiation energy E of 0.44 and 1670 J at ranges of 0.1 and 1 km, respectively.

2.2.2. Heterodyne detection

During heterodyne detection, the minimum detectable signal is

$$P_{\min} = \hbar\,c\,\Delta F / \eta\,\lambda\,, \quad (8)$$

where $\hbar$ is the Planck constant; c is the speed of light; η is the quantum efficiency of a detector of radiation. The necessary frequency bandwidth significantly narrows then, since one needs to detect the spectrum of beats between the detected and the emitted signals only, and $\Delta F = 10$ kHz. For $\eta = 0.1$, we find $P_{\min} = 3\cdot10^{-15}$ W.

In the heterodyne regime, the signal–to–noise ratio is

$$S / N = E\,A\,t\,\beta\exp(-2\alpha R)\,\eta\,\lambda / 2\,h\,\Delta F\,R^2 =$$

$$= 2\cdot10^8\ [\text{km}^2/\text{J}^{-1}]\,E\exp(-2\alpha R) / R^2. \quad (9)$$

At ranges of 0.1 and 1 km, we obtain $E_{\min} = 10^{-10}$ and $5\cdot10^{-5}$ J, respectively. Table I presents the characteristics of lidars used to implement the above measurement techniques.

The extinction of detected signal due to the CH_4 leaks may be accounted for using the data from Table II by the exponential factor and the factor of range, $\exp(-2\tau_b)/R^2$, where $\tau_b = N_b\,\sigma_{abs}\,R$; N_b is the background number density of methane.

TABLE I.

Lidar technique	Characteristics					
	ΔF, Hz	Photodetector	D^*, cm $\sqrt{\text{Hz}}$ / W	T, K	$\sqrt{S}$, mm	$P_{\min}$, W
Differential absorption	10^2	PbSe	10^9	293	1	10^{-9}
DAS, direct detection	$7.5\cdot10^6$	CdHgTe	$5\cdot10^{10}$	80	0.1	$5\cdot10^{-10}$
DAS, heterodyne detection	10^4	PbSe	10^9	293	1	$3\cdot10^{-15}$

TABLE II.

R, km	10^{-2}	$3.2\cdot10^{-2}$	10^{-1}	$3.2\cdot10^{-1}$	10^0	$3.2\cdot10^0$
$\exp(-2\tau_b)/R^2$	10^4	$7.8\cdot10^2$	$4.5\cdot10^1$	$8.0\cdot10^{-1}$	$3.4\cdot10^{-4}$	$7.6\cdot10^{-13}$

3. ELEMENTS OF THEORY OF CW LIDARS

To follow the frequency processing technique, a continuous signal is emitted into the atmosphere. Mostly, its carrier or subcarrier frequency is linearly modulated.[3] For an immobile target, the frequency of beats between the emitted and detected signals at range R will then be

$$f_R = 2\,R\,\Delta F\,F_m / c, \quad (10)$$

where ΔF is the frequency deviation and F_m is the modulation frequency.

The range resolution is specified as

$$\Delta R = c\,\Delta F_f / 4\,\Delta F\,F_m\,, \quad (11)$$

where ΔF_f is the filter transmission bandwidth. The value ΔR cannot be less than $\Delta R = c/4\Delta F$, i.e., it is controlled by frequency deviation. The minimum range is also dependent on ΔF only and found in exactly the same way. The rms methodological error of ranging is then

$$\sigma_R = c\,\Delta F_f / 8\sqrt{3}\,F_m\,\Delta F\,. \quad (12)$$

We proceed to estimate the parameters of the lidar prescribing the following values: $F_m = 200$ Hz, $\Delta F = 7.5$ MHz, $f_{\max} = 10$ kHz, $\Delta F_f = 400$ Hz. The

maximum range will then be R_{max} = 1 km. The minimum range and the step in ranging are R_{min} = 10 m. The potential resolution is ΔR = 10 m. The number of analyzer channels is n = 25. The rms methodological error is σ_R = 6 m.

3.1. Frequency instability and nonlinearity of modulation

We estimate the effect of instability of modulating subcarrier frequency and of nonlinearity of modulation upon the choice of modulation and accumulation period. It follows from Eq. (10) that the retrieval error of beat frequency due to instability of the subcarrier frequency is equal to

$$\Delta f_{R_{us}} = 4\,\Delta R_{us}\,\Delta F / c\,T_m\,, \qquad (13)$$

where ΔR_{us} is the ranging measurement error due to instability of the subcarrier frequency. On the other hand, the frequency instability $\Delta F_{us}/\Delta T$ over the time $2R/c$ may, at worst, produce a change in beat frequency of

$$\Delta f_{R_{us}} = 2\,R\,\Delta F_{us} / c\,\Delta T\,. \qquad (14)$$

It follows from Eqs. (13) and (14) that

$$\Delta F_{us} / \Delta T = 2\,\Delta R_{us} / R\,\Delta F / T_m\,. \qquad (15)$$

Therefore at the maximum range, the absolute instability over the period of modulation should not exceed the value

$$\Delta F_{us} \le 2\,\Delta R_{us} / R\,\Delta F / T_m\,. \qquad (16)$$

For definiteness, we set $\Delta R_{us} \le 0.1\,\Delta R$. Then

$$\Delta F_{us} \le 0.2\,\Delta R / R_{max}\,\Delta F\,. \qquad (17)$$

Consider the effect of nonlinearity of modulation of the subcarrier frequency on the accuracy of determination of current range. It follows from Eq. (10) that one should have for linear frequency modulation (LFM) $\Delta F/T_m = U_0$ = const. Apparently, $\Delta f_{Rnl} = 4R\Delta U/c$, where $\Delta U/U_0$ is the relative deviation from linearity (the relative nonlinearity). It is easy to find that $\Delta R_{nl} = R\Delta U/U_0$.

To define requirements for the linearity of frequency modulation, we set $\Delta R_{max\ nl} = 0.1\,\Delta R$. In that case

$$\Delta U / U_0 = 0.1\,\Delta R / R_{max}\,. \qquad (18)$$

4. EXPERIMENTAL PROTOTYPE OF GAS ANALYZER

The prototype of LFM IR lidar is capable of detecting the atmospheric inhomogeneities at ranges in excess of 100 m. The lidar (see Fig. 1) emitting unit includes two He–Ne lasers, *1* and *2*, both generating at 3.39 μm. Radiation is modulated by an electrooptic modulator built around a crystal of Ge, *3*. Detecting optics is constructed with a 1–m focus mirror telescope *6*, 150 mm in diameter. We use a thermoelectrically cooled PbSe photoresistor for an IR detector *7*. The spectrum analyzer *8* is at the output of photodetector. The output signals are detected, *9*, converted into digital form, *11*, and sended for algorythmic computer processing, *12*.

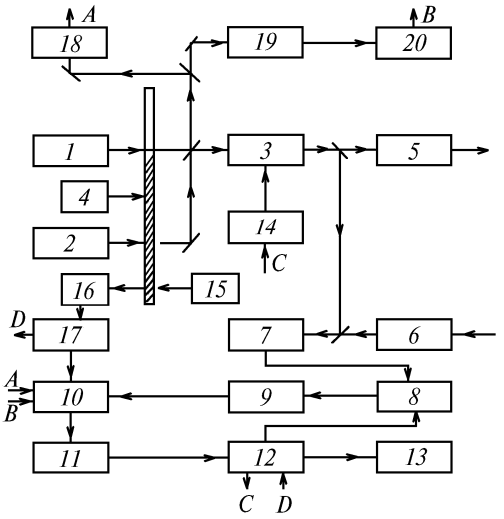

FIG. 1. Experimental prototype of lidar: He–Ne lasers (1 and 2); an electrooptic modulator (3); a chopper (4); a collimator (5); a telescope (6); a PbSe photoresistor (7); a spectrum analyzer (8); a detector (9); a multiplexor (10); an analog–to–digital converter (11); a microcomputer (12); a display (13); a LFM generator (14); a light diode (15); a Ge photodiode (16); a synchronizer (17); pirodetectors (18 and 20); and, CH_4 *cell (19).*

CONCLUSION

The described system appears to be quite attractive, since a continuous–wave gas lasers are several tens of times cheaper than a pulse solid lasers. Therefore, research and development in cw–laser systems may open new prospects for remote monitoring of the atmosphere, e.g., by the techniques of laser–induced fluorescence, differential absorption and scattering, etc.

REFERENCES

1. Yu. E. Pol'skii, Opt. Atm. **1**, No. 8, 3–13 (1988).
2. R.R. Agishev, *Protection Against Background Interference in Optoelectronic Systems of Atmospheric Monitoring* (Mashinostroenie, Moscow, 1994), 128 pp.
3. R.R. Agishev, L.R. Aibatov, A.N. Ivanov, G.I. Il'in, and Yu.E. Pol'skii, in: *Abstracts of Reports at the 9th All–Union Symposium on Laser and Acoustic Sensing of the Atmosphere,* Tomsk (1987), Vol. 2, pp. 112–116.
4. A.I. Popov and A.V. Sadchikhin, Zh. Prikl. Spectrosk. **55**, No. 3, 426–430 (1991).
5. R.M. Abdullin, S.A. Boiko, S.B. Kotel'nikov, and A.I. Popov, in: *Proceedings of the 15th International Laser Radar Conference*, Tomsk (1990), Vol. 2, pp. 108–112.
6. R.M. Measures, *Laser Remote Sensing* (John Willey and Sons, N.Y., 1987).
7. E.Hinkley, ed., *Laser Monitoring of the Atmosphere* (Springer Verlag, New York, 1976).
8. N.S. Kopeika and J. Borodona, Proc. IEEE **58**, No. 10, 1571–1577 (1970).
9. D.K. Barton and H.R. Ward, *Handbook of Radar Measurements* (New Jersey, Prentice–Hall, 1969).
10. K.F. Hulme, Opt. and Laser Technology **14**, No. 4, 213–215 (1982).